

6th International Conference on Silicon Photovoltaics, SiliconPV 2016

## Extraction of recombination properties from lifetime data

Gaby J.M. Janssen<sup>a\*</sup>, Yu Wu<sup>a</sup>, Kees C.J.J. Tool<sup>a</sup>, Ingrid G. Romijn<sup>a</sup> and Andreas Fell<sup>b†</sup><sup>a</sup>ECN Solar Energy, Westerduinweg3, 1755LE Petten, The Netherlands<sup>b</sup>The Australian National University, 0200 Canberra, Australia

---

**Abstract**

Extraction of recombination properties like the recombination pre-factor  $J_0$  and the Shockley-Read-Hall base lifetime from photoconductance data on test structures and half-fabricates of photovoltaic cells is not always straightforward and unambiguous. In this paper the well-known “slope method” of Kane and Swanson will be compared to the method offered by the Quokka code. The Quokka code numerically solves the distribution of the excess carrier concentration over the thickness of the wafer at several injection levels. In this way artefacts due to transport limitations are avoided and the analysis does not rely on data at a single injection level. This gives more reliable results for  $J_0$  and the base lifetime. A method to determine the base lifetime from the implied  $V_{OC}$  at 1 Sun illumination values is also presented.

© 2016 Published by Elsevier Ltd. This is an open access article under the CC BY-NC-ND license

(<http://creativecommons.org/licenses/by-nc-nd/4.0/>).

Peer review by the scientific conference committee of SiliconPV 2016 under responsibility of PSE AG.

**Keywords:** silicon photovoltaic cells; recombination; lifetime; dark saturation current; QSSPC.

---

**1. Introduction**

Solar cell optimization requires good, quantitative knowledge of the recombination parameters in a cell. These are e.g. the recombination pre-factor  $J_0$  of the diffused regions and  $\tau_{SRH}$ , the Shockley-Read-Hall lifetime of the base. The Sinton WTC-120 lifetime tester is a convenient and fast instrument that from quasi steady state photoconductance (QSSPC) measurements provides the effective lifetime  $\tau_{eff}$  for a range of excess carrier densities

---

\* Corresponding author. Tel.: +31 – 88 515 4803

E-mail address: [janssen@ecn.nl](mailto:janssen@ecn.nl)

† Present address: Fraunhofer Institute for Solar Energy Systems, 79110 Freiburg, Germany

$\Delta n$  [1]. From these data the recombination parameters  $J_0$  and  $\tau_{SRH}$  can be extracted. The conventional method to do this is the slope method by Kane and Swanson [2]. This method has been implemented in the Sinton WTC-120 software. Recently this method was adapted to partially account for bandgap narrowing that occurs in the base at high injection levels [3].

The Kane and Swanson method has been proven to be very useful for extraction of  $J_0$  data. Values of the base lifetime  $\tau_{SRH}$  extracted by this method are usually not reported. The  $\tau_{SRH}$  is usually determined from measurements on structures where diffused regions have been stripped off and subsequently given an excellent surface passivation. While this method gives reproducible data, it gives only limited information of any impact the diffusion processes may have on the  $\tau_{SRH}$ . One reason why the  $\tau_{SRH}$  values by the Kane and Swanson are not often reported may be that they depend strongly on the selected point of analysis and that the  $\tau_{SRH}$  values are much more sensitive to this selection than the  $J_0$  values. This often results in a large scatter of the  $\tau_{SRH}$  values.

There are several causes for this strong dependence on the selected point of analysis.

- The carrier dependency of  $J_0$  and  $\tau_{SRH}$  itself. According to the Shockley-Read-Hall (SRH) theory the  $\tau_{SRH}$  of the base will vary with the injection level depending on the relative values of the capture time constants  $\tau_{0p}$  and  $\tau_{0n}$  [4]. This transition takes place when going from low level injection conditions to high level injection and is usually within the injection level range where lifetime data are taken. Also the  $J_0$  will be carrier dependent, e.g. due to the non-uniform quasi-Fermi levels in the diffused regions at high injection, or due a breakdown of field-induced surface passivation at high injection levels [5].
- Bandgap narrowing in the base. The effect of bandgap narrowing in the base was recognized by Kimmerle et al. [3]. The authors proposed a correction which was recently implemented in the standard Sinton WTC-120 software.
- A non-uniform distribution of the carrier density in the sample that increases with injection level. This occurs e.g. in samples with a high  $J_0$  because of transport limitations [6-8]. These transport limitations cause  $\Delta n$  values at the interfaces of the base and the heavily doped region to be lower than the average  $\Delta n$ . This results in an apparent decrease of  $J_0$  with the injection level.

In this paper we will compare the standard Kane-Swanson slope method and recent modifications with the Quokka method presented by Fell et al. [9,10]. The Quokka code is used to calculate the effective lifetime in a sample by numerical solving the distribution of  $\Delta n$  over the base. In this way transport limitations are included. In this paper the method using Quokka will be demonstrated further for test structures and half-fabricates with the emphasis on determining the  $\tau_{SRH}$ . Furthermore we will demonstrate that by using the implied  $V_{oc}$  values at one sun illumination the scatter often observed in the  $\tau_{SRH}$  is already significantly reduced.

## Nomenclature

$G$	total photogeneration rate
$J_0$	recombination prefactor, with subscripts front, rear or base to designate region of origin
$J_{ph,1Sun}$	generated photocurrent at 1 Sun illumination
$\Delta n$	excess carrier concentration
$N_D$	doping concentration of the base material
$n_i$	intrinsic carrier concentration
$n_{i,eff}$	intrinsic carrier concentration with correction for bandgap narrowing
$q$	magnitude of elementary charge
$S$	surface recombination velocity
$W$	thickness of the wafer
$\tau_{eff}$	effective lifetime in the base material
$\tau_{SRH}$	Shockley-Read-Hall lifetime
$\tau_{0p}$	capture time constant of holes
$\tau_{0n}$	capture time constant of electrons
$\tau_{intr}$	intrinsic lifetime associated with radiative and Auger recombination in the base
$\tau_{corr}$	effective lifetime after correction for intrinsic lifetime

## 2. Methods

### 2.1. The Kane and Swanson slope method

This method is implemented in the WTC-120 software [1]. It assumes that at each excess carrier concentration  $\Delta n$  the total recombination can be expressed by:

$$\frac{\Delta n}{\tau_{eff}} = \frac{\Delta n}{\tau_{intr}} + \frac{\Delta n}{\tau_{SRH}} + \frac{J_0(N_D + \Delta n)\Delta n}{qWn_i^2} \quad (1)$$

Here  $W$  is the thickness of the sample,  $N_D$  the base doping concentration,  $n_i$  the intrinsic carrier density and  $\tau_{intr}$  the lifetime associated with radiative and Auger recombination in the base.  $J_0$  is obtained from the slope of  $1/\tau_{corr} = (1/\tau_{eff} - 1/\tau_{intr})$  versus  $\Delta n$ . The  $\tau_{SRH}$  is obtained as the value of the linear approximation at  $\Delta n = -N_D$ . As in practice a plot of the inverse corrected lifetime versus  $\Delta n$  is not always a straight line, a small range of  $\Delta n$  values is selected. This makes the analysis somewhat arbitrary. As mentioned above this deviation of a straight line is partly due to the band gap narrowing which causes  $n_i^2$  to be dependent on  $\Delta n$  [3]. Implementing this in equation (1) leads to:

$$\frac{d}{d(\Delta n)} \left( \frac{n_{i,eff}^2}{\tau_{corr}} \right) = \frac{J_0}{qW} + \frac{d}{d(\Delta n)} \left( \frac{n_{i,eff}^2}{\tau_{SRH}} \right) \quad (2)$$

In the most recent version of the Sinton WTC-120 software this equation is used with  $n_{i,eff}^2$  calculated using Schenk's model [11]. The last on the right hand side is neglected. However, Kimmerle showed that by using an iterative method this term can accurately be accounted for [7]. This approach has the added benefit that  $\tau_{SRH}$  is not obtained from an extrapolation of the fit point to  $\Delta n = -N_D$  but uses lifetime data in the range where  $J_0$  is fitted. Kimmerle also proposed a method that analytically accounts for charge carrier transport limitations.

### 2.2. Calculating $\tau_{SRH}$ from implied $V_{OC}$

The WTC-120 software explicitly supplies the implied  $V_{OC}$  value at one sun illumination, which is in fact another representation of  $\Delta n$  at one sun illumination. This allows for extraction of an effective " $J_{0,base}$ " at 1 Sun and the corresponding base lifetime  $\tau_{SRH}$ :

$$iV_{OC} = \frac{kT}{q} \ln \left( \frac{J_{ph,1Sun}}{J_0 + J_{0,base}} + 1 \right) \quad \text{and} \quad \tau_{SRH} = \frac{qWn_i^2}{J_{0,base}(N_D + \Delta n_{1Sun})} \quad (3)$$

$J_{ph,1Sun}$  is the total generation at 1 Sun, which can be calculated using the optical constant used for the lifetime measurement [1].  $\Delta n_{1Sun}$  can be calculated from the  $iV_{OC}$  at one sun. Note that " $J_{0,base}$ " is not a proper  $J_0$  in the sense that it does not represent recombination with ideality factor equal one at high injection.  $J_{0,base}$  only reflects the SRH recombination contribution at one sun illumination. At constant  $\tau_{SRH}$  this contribution decreases with injection level. The method of calculating  $\tau_{SRH}$  from implied  $V_{OC}$  requires a reliable value of  $J_0$  obtained e.g. by the slope method, preferably corrected for bandgap narrowing. Like the analysis of Kimmerle [7], it replaces the extrapolation to  $\Delta n = -N_D$  by an extrapolation to data closer to the actual operation of the solar cell. It has the advantage of being easy to calculate based on the present output from the Sinton WTC-120 software. Note, that  $\tau_{SRH}$  calculated according to eq. 3 contains SRH and intrinsic recombination. For wafers with diffused surfaces at 1 Sun illumination the intrinsic recombination in the base is a minor contribution.

### 2.3. The Quokka method

The Quokka code numerically solves the distribution of the excess carrier density  $\Delta n$  in the base of solar cell in a steady state at a given illumination and voltage bias. The approach using Quokka is similar to the one proposed by

Thomson although Quokka is steady-state only and the method by Thomson solves the time dependent-equations consistent with the transient mode of the Sinton lifetime tester [12]. However, Thomson et al. did not discuss on finding the base recombination parameters.

The recombination and conduction properties of passivated surfaces, either lightly or heavily doped, and contacts are treated as boundary conditions. This focus on the excess carrier density in the base makes Quokka well suited to analyze QSSPC lifetime data which rely on a measurement of the average excess carrier density in the base. The Quokka method assigns a  $J_{0,front}$  and  $J_{0,rear}$  value to the front and rear of a test structure. The sum of these would be equivalent to  $J_0$  of eq. 1. Alternatively, for non-doped surfaces an effective surface combination value can be supplied. The base recombination is characterized by  $\tau_{SRH}$ , or by  $\tau_{op}$  and  $\tau_{on}$ . This allows for an increase of the base life time with injection level. The radiative and Auger recombination in the base are calculated using recent models [13]. Quokka includes part of the bandgap narrowing in the base due to doping level by the model of Schenk [11]. The carrier density distribution over the base is numerically calculated at open-circuit conditions and with a fixed generation profile with total generation rate  $G$ . The effective life time is obtained from the averaged  $\Delta n$  over the base:  $\Delta n_{av}/\tau_{eff} = G$ . This process can be repeated for different values of  $G$ , i.e. different injection levels. An optimization routine is supplied to find the recombination parameters that best fit the lifetime curve. In practice, the recombination processes in the test samples considered contain only variation with either  $\Delta n$  or  $\Delta n^2$ . Therefore the choice of parameters to be optimized is essentially limited to two, although there is no strict limit imposed. Useful choices are e.g.

- $J_{0,front} = J_{0,rear}$  and either  $\tau_{SRH}$  or  $\tau_{op}$  with  $\tau_{op} = \tau_{on}$  in the case of a symmetrical test structure.
- One value of the pair  $J_{0,front}$ ,  $J_{0,rear}$  with the other one fixed, and either  $\tau_{SRH}$  or  $\tau_{op}$  with  $\tau_{op} = \tau_{on}$  for asymmetrical test structures such as half fabricates of front and rear contacted solar cells.
- Either a surface recombination velocity  $S$  or the base recombination parameters as above for test structures without heavily doped surfaces.

The Quokka method assumes  $n_i = 9.65 \cdot 10^9 \text{ cm}^{-3}$  for intrinsic silicon at 300 K. Values were rescaled to  $n_i = 8.6 \cdot 10^9 \text{ cm}^{-3}$  which is the value adopted by the Sinton WTC-120 software and close to the expected  $n_i$  value at 298 K.

### 3. Experiment

The lifetime samples considered in this study were of type p+/n/p+ or of type p+/n/n+. A small set, denoted set I, was made from textured Cz-wafers with a relatively low doping concentration of  $9.2 \cdot 10^{14} \text{ cm}^{-3}$ . These were exposed to either just a BBr<sub>3</sub> diffusion process or to both a BBr<sub>3</sub> (resulting sheet resistance 60  $\Omega/\text{sq}$ ) and POCl<sub>3</sub> (sheet resistance 20  $\Omega/\text{sq}$ ) diffusion process, with subsequent SiN<sub>x</sub> passivation. A second set, denoted set II, consisted of five groups of ten p+/n/n+ half fabricates each made from textured Cz wafers with a base doping of  $2.4 \cdot 10^{15} \text{ cm}^{-3}$ . The five groups all had a boron and an a phosphorus diffused surface with SiN<sub>x</sub> passivation but had seen slightly different processing conditions. In this set the half fabricates were targeted towards similar  $J_0$  at front and rear. Lifetime measurements were done with the Sinton lifetime WTC-120 tester.

### 4. Results

#### 4.1. Results set I

As typical examples Fig. 1 shows the effective lifetime curves of a symmetric p+/n/p+ structure and an asymmetric p+/n/n+ structure in which one of the sides is much more heavily doped than the other. Fig. 1 also shows the data points from a Quokka fit, with  $\tau_{op} = \tau_{on}$ . For both structures there is excellent agreement with the experimental data, corresponding to an  $R^2$  value of the fit exceeding 0.99. Fig. 2 compares the  $J_0$  values that were obtained with values obtained by the slope method at various excess carrier density values and by the diffusion corrected method proposed by Kimmerle et al. [7].

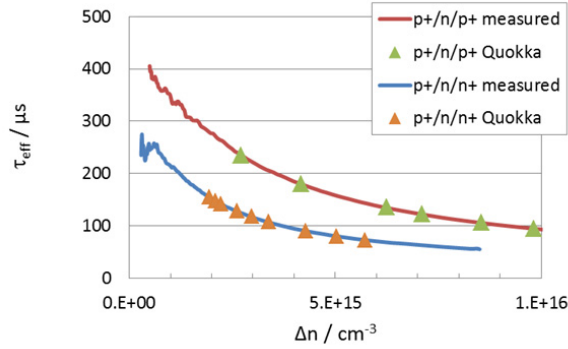


Fig. 1. Measured lifetime curves of p+/n/p+ and p+/n/n+ structures with points fitted by Quokka

The  $J_0$  values obtained for the symmetrical samples are close together, with the exception of values obtained at the low injection level of  $2 \cdot 10^{15} \text{ cm}^{-3}$ , a level usually considered too low for a meaningful separation of recombination of ideality one and two. Also note that for these  $J_0$  values the diffusion correction is only minor. In the case of an asymmetrical sample with one heavily doped surface, the slope method as expected shows a decrease of the apparent  $J_0$  value with injection level. This decrease is less pronounced when using the diffusion correction, but compared to the Quokka method the total  $J_0$  still seems underestimated. The present form of the diffusion corrected method treats the sample as symmetrical, whereas the Quokka method can incorporate the asymmetry in the boundary conditions and hence in the carrier density profile. Ignoring this asymmetry results in a serious underestimation of the  $J_0$  of the heavily doped surface.

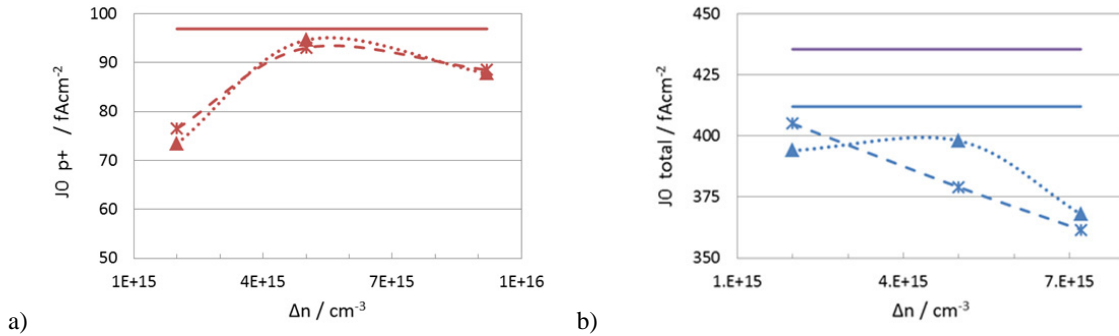


Fig. 2.  $J_0$  values determined for the a) p+/n/p+ structure and b) p+/n/n+ structure. Asterisks: slope method, triangles: diffusion corrected method, solid line: Quokka method. In b) the blue line was obtained by treating the sample as symmetrical, the purple line corresponds to an asymmetrical configuration.

The calculated base lifetimes of both structures are shown in Fig. 3a and Fig. 3b. According to the Quokka analysis the experimental data agrees very well with the assumption of a constant  $J_0$  of Fig. 2, defining the recombination at the surfaces, and a  $\tau_{SRH}$  that slightly increases with injection level. The slope method and the diffusion corrected method on the other hand give a large scatter in  $\tau_{SRH}$  results. The Quokka analysis assumed  $\tau_{op} = \tau_{on}$ . A higher  $\tau_{op}/\tau_{on}$  ratio would involve a smaller increase of  $\tau_{SRH}$  with  $\Delta n$ , and would slightly reduce the resulting  $J_0$ . Part of the small discrepancy found here between the  $J_0$  of the Quokka method and the other methods could be due to this effect.

Also indicated in Fig. 3a is the lifetime obtained by using the  $iV_{OC}$  at 1 Sun value reported by the Sinton lifetime software. As stated above this requires reliable  $J_0$  data obtained by the slope method. Here the diffusion corrected value of  $J_0 = 87.8 \text{ fAcm}^{-2}$  per surface was used resulting in  $J_{0,base} = 45.6 \text{ fAcm}^{-2}$ . As appears from Fig. 3a the method

results in a value somewhat higher than the Quokka value for the symmetrical sample. In the case of the p+/n/ n+ structure a similar approach resulted in  $J_{0,base} < 5 \text{ fAcm}^{-2}$ , which is too low for a meaningful calculation of the  $\tau_{SRH}$ .

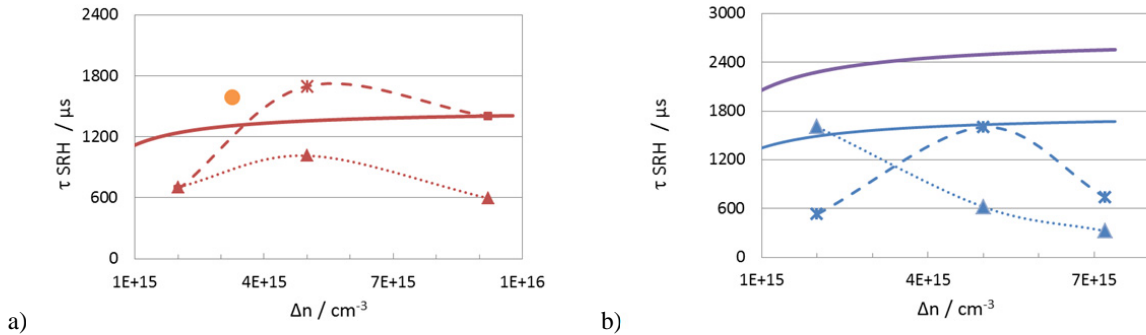


Fig. 3  $\tau_{SRH}$  values determined for determined for a) p+/n/p+ structure and b) p+/n/n+ structure. Asterisks: slope method, triangles: diffusion corrected method, solid line: Quokka method. In a) the dot indicates the lifetime derived from the  $iV_{OC}$ . In b) the blue solid line was obtained by treating the sample as symmetrical, the purple solid line corresponds to an asymmetrical configuration.

#### 4.2. Results set II

Fig. 4 shows  $J_0$  results for the larger data set II which allows to inspect statistical variations in the analysis results. The slope analysis was done at a suboptimal, low injection level of  $\Delta n = 2 \cdot 10^{15} \text{ cm}^{-3}$ . The diffusion correction method was applied in the suggested optimal range of  $1\text{--}2 \cdot 10^{16} \text{ cm}^{-3}$ . The Quokka analysis was in the range  $3\text{--}10 \cdot 10^{15} \text{ cm}^{-3}$ . The  $J_0$  values of the various methods show some systematic differences over all the groups with the diffusion corrected values lower than the Quokka values. But it should be noted that the standard deviations both of the  $J_0$  values by the diffusion corrected and the Quokka method are much smaller than by the slope method. There is one exception, group D, where the Quokka method actually shows a large scatter and the average values differ more among each other than in other groups. This could also be correlated to a poorer fit of the Quokka method, i.e. of  $R^2 < 0.99$ , which did not occur in other groups. This illustrates that the Quokka method can detect cases where the analysis method may not be adequate or data is spurious.

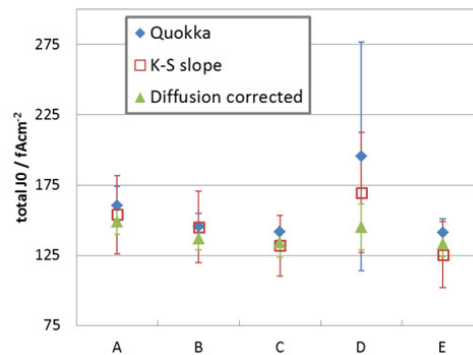


Fig. 4.  $J_0$  determined according to the slope method, the diffusion corrected method and the Quokka method of five groups of p+/n/n+ test structures. Data points are averages over 10 measurements per group and error bars correspond to the standard deviation.

The calculated  $\tau_{SRH}$  of this set are shown in Fig 5. This shows firstly that the lifetimes based on the intercept of the slope at  $\Delta n = -N_D$  have very large variations and that the average values can differ substantially from the average values obtained with the other methods. It should be noted that even with the alternative methods standard deviations of the  $\tau_{SRH}$  are relatively much larger than of the  $J_0$  values.

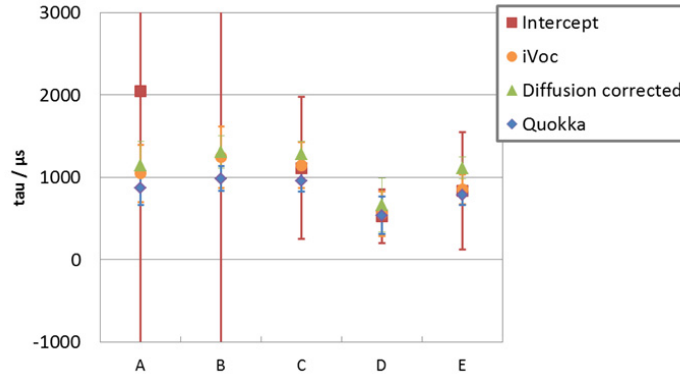


Fig. 5.  $\tau_{SRH}$  from intercept,  $iVoc$  @ 1 Sun, the diffusion corrected method and the Quokka method of 5 groups of p+/n/n+ test structures. Data points are averages over 10 measurements per group and error bars correspond to the standard deviation. For group B the intercept value is off-scale at 8000  $\mu s$ .

## 5. Discussion

All methods discussed in this paper are based upon the separation of recombination scaling with  $\Delta n$  or with  $\Delta n^2$ . This also implies that only two independent parameters can be obtained. Although they are usually identified with  $J_0$  of the doped surface and  $\tau_{SRH}$  of the base, they represent the total recombination with ideality one, respectively ideality two, at high level injection. This means that  $\tau_{SRH}$  can contain  $p$ - $n$  junction recombination or that  $J_0$  can be SRH recombination from a lightly doped base surface in strong inversion or accumulation conditions.

The Quokka method, like the method presented by Thomson [12] but at contrast with other analyses, does not use a differential method to obtain the parameters but fits large part of the  $\tau_{eff}$  versus  $\Delta n$  curve. This seems in particular beneficial for the  $\tau_{SRH}$  which is now treated as a real fit parameter instead of the residual of the differential method. Moreover, by using  $\tau_{op}$  as parameter with a fixed  $\tau_{op}/\tau_{0n}$  ratio a slight increase of  $\tau_{SRH}$  with  $\Delta n$  can be included, consistent with SRH theory.

Both the diffusion corrected analysis and the Quokka method are suited to deal with a non-uniform carrier density concentration due to transport limitations. In addition, Quokka can handle asymmetric structures, as long as at one side  $J_0$  is assumed known or the ratio  $J_{0, rear}/J_{0, front}$  is constant. However, it seems that when  $J_0$  is smaller than 100 fA/cm<sup>2</sup> per side, transport limitations have a minor impact.

The drawback of Quokka is that it requires a numerical simulation which takes about 1-2 minutes per curve on an average laptop. For routine inspection of large data sets of samples with similar front and rear  $J_0$  the diffusion corrected method seems adequate. When transport corrections are small, the analysis can be based upon the standard slope method including band gap narrowing. In those cases extracting the  $\tau_{SRH}$  from the  $J_0$  and the  $iV_{OC}$  value seems to be preferable over the intercept value, as it involves extrapolation over a smaller  $\Delta n$  range and uses actual data points close the operation point of a solar cell.

It should be noticed however, that the  $J_{0, base}$  calculated according to eq. 3 should be larger than the error in  $J_0$  of the surfaces. In practice, when  $J_{0, base} < 10$  fAcm<sup>-2</sup> the corresponding  $\tau_{SRH}$  cannot be trusted. However, it applies to all analyses methods discussed that  $J_0$  or  $\tau_{SRH}$  will only be significant when they have a substantial impact on the life time curve. In the cases where one parameters dominates, the other is not reliable.

## 6. Conclusions

- The Quokka method is well suited to extract  $J_0$  and, in particular,  $\tau_{SRH}$  values from  $\tau_{eff}$  versus  $\Delta n$  curves.
- Transport limitations causing non-uniform  $\Delta n$  over the base are accounted for in the Quokka method, which is significant for heavily doped surface regions. This is also adequately treated by the diffusion correction method but Quokka can handle certain cases of asymmetry in the sample.

- When the slope method is used to extract  $J_0$ , calculating the base lifetimes from  $iV_{OC}$  is more reliable as large extrapolations are avoided and an additional data point is used.

Application of the methods presented here will give more reliable data on  $J_0$  and the SRH lifetime of silicon photovoltaic cells. This is required to steer optimization of current industrial manufacturing of cells to > 21% efficiency.

## Acknowledgements

The authors would like to thank Achim Kimmerle of Fraunhofer ISE for providing them with a spreadsheet containing the beta-version of his method for carrier diffusion corrected analysis.

## References

- [1] Sinton R, Macdonald D, WCT-120 Photoconductance Lifetime Tester and optional Suns-VOC Stage User Manual. Boulder, Colorado: Sinton Consulting, Inc; 2006.
- [2] Kane DE, Swanson RM, Measurement of the emitter saturation current by a contactless photoconductivity decay method, 18th IEEE Photovoltaic Specialists Conference, Las Vegas: 1985. p. 578.
- [3] Kimmerle A, Rothhardt P, Wolf A, Sinton RA. Increased Reliability for  $J_0$ -analysis by QSSPC. Energy Procedia 2014; 55:101-6.
- [4] Aberle AG, Crystalline Silicon Solar Cells; Advanced Surface Passivation and Analysis. Center for Photovoltaic Engineering, University of New South Wales, Sydney, Australia; 1999.
- [5] Duttagupta S, Ma FJ, Hoex B, Aberle AG. Excellent surface passivation of heavily doped p+ silicon by low-temperature plasma-deposited SiO<sub>x</sub>/SiN<sub>y</sub> dielectric stacks with optimised antireflective performance for solar cell application. Solar Energy Materials and Solar Cells 2014; 120:204-8.
- [6] Cuevas A, Macdonald D. Measuring and interpreting the lifetime of silicon wafers. Sol. Energy 2004; 76:255-62.
- [7] Kimmerle A, Greulich J, Wolf A. Carrier-diffusion corrected  $J_0$ -analysis of charge carrier lifetime measurements for increased consistency. Solar Energy Materials and Solar Cells 2015; 142:116-22.
- [8] Min B, Dastgheib-Shirazi A, Altermatt PP, Kurz H. Accurate determination of the emitter saturation current density for industrial p-diffused emitters, 29th European Photovoltaic Solar Energy Conference, Amsterdam: 2014.
- [9] Fell A. A Free and Fast Three-Dimensional/Two-Dimensional Solar Cell Simulator Featuring Conductive Boundary and Quasi-Neutrality Approximations. IEEE Transactions on Electric Devices 2013; 60:733-8.
- [10] Fell A, McIntosh KR, Abbot M, Walter D, Quokka version 2: selective surface doping, luminescence modeling and data fitting, 23rd Photovoltaic Science and Engineering Conference (PVSEC), Taipei: 2013.
- [11] Schenk A. Finite-temperature full random-phase approximation model of band gap narrowing for silicon device simulation. J. Appl. Phys. 1998; 84:3684-95.
- [12] Thomson A, Grant N, Chern KF, Kho T. Improved Diffused-region Recombination-current Pre-factor Analysis. Energy Procedia 2014; 55:141-8.
- [13] Richter A, Glunz SW, Werne F, Schmidt J. Improved quantitative description of Auger recombination in crystalline silicon. Physical Review B: Condensed Matter & Materials Physics 2012; 86:1-14.